



Article

Finite-Time Synchronization Criteria for Caputo Fractional-Order Uncertain Memristive Neural Networks with Fuzzy Operators and Transmission Delay Under Communication Feedback

Hongguang Fan ^{1,2,3} , Kaibo Shi ⁴ , Zizhao Guo ^{5,*} and Anran Zhou ¹

¹ College of Computer, Chengdu University, Chengdu 610106, China; fanhongguang@cdu.edu.cn (H.F.); zhouanran@cdu.edu.cn (A.Z.)

² Key Laboratory of Pattern Recognition and Intelligent Information Processing, Institutions of Higher Education of Sichuan Province, Chengdu University, Chengdu 610106, China

³ School of Mathematical and Computational Science, Hunan University of Science and Technology, Xiangtan 411201, China

⁴ School of Electronic Information and Electrical Engineering, Chengdu University, Chengdu 610106, China; shikaibo@cdu.edu.cn

⁵ Shenzhen Institute for Advanced Study, University of Electronic Science and Technology of China, Shenzhen 610056, China

* Correspondence: jiaoxi@cdu.edu.cn

Abstract: Unlike existing memristive neural networks or fuzzy neural networks, this article investigates a class of Caputo fractional-order uncertain memristive neural networks (CFUMNNs) with fuzzy operators and transmission delay to realistically model complex environments. Especially, the fuzzy symbol AND and the fuzzy symbol OR as well as nonlinear activation behaviors are all concerned in the generalized master-slave networks. Based on the characteristics of the neural networks being studied, we have designed distinctive information feedback control protocols including three different functional sub-modules. Combining comparative theorems, inequality techniques, and stability theory, novel delay-independent conditions can be derived to ensure the finite-time synchronization (FTS) of fuzzy CFUMNNs. Besides, the upper bound of the settling time can be effectively evaluated based on feedback coefficients and control parameters, which makes the achievements of this study more practical for engineering applications such as signal encryption and secure communications. Ultimately, simulation experiments show the feasibility of the derived results.

Keywords: fuzzy operator; control technique; synchronization requirement; Caputo derivative; neural network



Citation: Fan, H.; Shi, K.; Guo, Z.; Zhou, A. Finite-Time Synchronization Criteria for Caputo Fractional-Order Uncertain Memristive Neural Networks with Fuzzy Operators and Transmission Delay Under Communication Feedback. *Fractal Fract.* **2024**, *8*, 619. <https://doi.org/10.3390/fractalfract8110619>

Academic Editors: Feifei Du and Wang Fei

Received: 11 September 2024

Revised: 14 October 2024

Accepted: 22 October 2024

Published: 23 October 2024



Copyright: © 2024 by the authors. Licensee MDPI, Basel, Switzerland. This article is an open access article distributed under the terms and conditions of the Creative Commons Attribution (CC BY) license (<https://creativecommons.org/licenses/by/4.0/>).

1. Introduction

With the advancement of modern intelligence theory and software program technology, multifarious neural networks (NNs) consisting of multilayer neurons have attracted increased interest from scientific personnel because of their powerful adaptability, good fault tolerance, adjustable topological structure, and superior parallel computing competence [1–5]. Numerous intensive studies have shown that NNs can simulate human brain thinking and have prospective utilizations in different fields, such as computational neuroscience [6], secure processing [7], parameter optimization [8], intelligent detection [9], and stability analysis [10–12]. Synchronization, as a significant characteristic dynamic behavior of complex systems and NNs, has succeeded in generating a wide range of academic discussions [13–15]. So far, there are several dominant synchronization modes, such as μ -synchronization [16], projective synchronization [17], event-triggered synchronization [18], and finite-time synchronization [19–21].

Memristors, as the best hardware for effectuating neuronal synaptic functions in neural networks, have a rapid rate of cross-array calculation. Engineers and researchers applied memristors to neural networks and established various memristive neural networks

(MNNs) with different application backgrounds. For instance, in [22], Bao et al. considered the nonlocal synchronization for MNNs with stochastic Wiener process and variable impulsive delay by Lyapunov methods and system stabilization. In [23], Sun et al. designed a class of nonlinear MNNs framework that can achieve delayed associative memory and utilized circuit simulation to realize the functions of fast learning and slow forgetting, providing a valuable research idea for the advancement of neuromorphic systems. In [24], a novel memristive state neural network was built using the least mean square algorithm and online learning techniques. This innovative achievement provided a distinctive perspective for devising neuromorphic computational networks. Under the balanced diagram framework, Ding et al. [25] considered the synchronization and anti-synchronization tasks for MNNs with proportional delays of unknown bounds through the self-triggered technique and parameter variation approach. By a concise and efficient information feedback mechanism, Hua et al. [26] paid attention to the nonlocal synchronization challenge of multi-layer MNNs with multiple delays based on the approach of system solutions. By the nonlinear scalarization method, Li et al. [27] discussed the nonlocal synchronization for nonlinear quaternion-valued MNNs with uncertain interferences.

It should be noted that the MNN models and synchronization applications mentioned above mainly rely on traditional calculus operators. Fractional calculus, as a generalized form of integer calculus, possesses an addition parameter and more historical information from the starting moment to the current moment [28]. Comparing and analyzing the two operators, the fractional form has the merits of being non-locality and memory, allowing for a more accurate display of actual phenomena such as physical elasticity, non-rigid motion, and heat transfer. Up to now, many researchers have applied fractional order calculus to neural network modeling and synchronization problems. To mention a few, in [29], Bao et al. established fractional Caputo-type MNNs with constant delay in the sense of Filippov and obtained judgment conditions to ensure that the master-slave network systems completed the synchronization through an adaptive feedback algorithm. In [30], Liu et al. deliberated a kind of uncertain fractional-order MNNs and analyzed their robust synchronization conditions by closure arithmetic and fractional stability theory. Utilizing the Riemann-Liouville operator instead of the Caputo operator, Gu et al. [31] explored the global synchronization of fractional MNNs including unknown factors, and derived a parameter recognition method by adaptive mechanism. With the help of the fractional comparison principle, the authors constructed a mixed loop controller for realizing the nonlocal synchronization objective of multi-delay NNs with memristive features [32]. By establishing new fractional comparison inequality, Fan et al. [33] investigated a class of generalized nontraditional projection synchronization for fractional-order uncertain MNNs through the hybrid loop feedback scheme and impulsive sampling information. More recent attention to synchronization control and analysis of memristor-based NNs with fractional order can be found in the literature [34–37].

Regarding real applications in uncertain and complex environments, NNs are generally modeled with soft thresholds and fuzzy calculations. Fuzzy logic theory, as a soft computing mechanism based on human thinking, can describe and handle various uncertainties and fuzzy problems. By fuzzy operators OR and AND, in [38], Li et al. constructed a kind of fractional-order delayed fuzzy NNs, and deduced network quasi-synchronization case through the nabla convolution and nonlinear feedback function. In [39], asymptotic synchronization circumstances of fractional-order NNs involving fuzziness and variable delays were derived by means of a discrete-time control scheme and Caputo differential inequalities. By the Laplace transform and comparative inequalities, Du et al. [40] solved the FTS of fractional-order NNs with fuzzy operations via adaptive control laws. Afterwards, in [41], the practical FTS conditions for fuzzy cellular NNs with Caputo operators were derived and the consequential upper bound of stable time was estimated. Expanding variables from the real number range to the complex number range, Jin et al. [42] constructed complex-valued fuzzy NNs with multiple delays and evaluated the settling time of network synchronization. Note that the fuzzy neural network models in [38–42] did not take into

account the memristive characteristics and uncertain links. Combining fuzzy operators and memristors in neural networks can better simulate real-world uncertain environments. To our knowledge, few studies have considered the FTS problem for fractional-order uncertain memristor-based NNs with fuzzy operators and transmission delay by delayed and non-delayed information feedback mechanisms, which constitutes the main intention of this article.

Enlightened by the above results and analysis, this study discusses the FTS for fuzzy CFUMNNs with transmission delay. The principal research highlights comprise three parts. First, memristive features, fuzzy operators, transmission delay, and uncertain weights are all considered for modeling real fractional-order NNs, which expands the relevant works [30–37] without fuzziness, and [38–42] without memristors. Second, different from the control schemes in [19–21], novel discontinuous information feedback control protocols are designed, which consist of three different functional sub-modules for eliminating the quasi-linear growth error, overcoming the time-delay effect, and implementing the synchronization task. Lastly, novel sufficient delay-independent conditions can be derived to ensure the FTS of fuzzy CFUMNNs based on information feedback schemes and various inequality techniques. Additionally, the settling time bound can be effectively evaluated based on feedback coefficients and control parameters, making our achievements more practical for engineering applications.

2. Fractional Knowledge and Mathematical Models

This part gives some related concepts, assumptions, and prominent results about fractional calculus. Then, fractional-order master-slave MNN models are built in complex situations.

Definition 1. Define fractional integral of a function $\mathcal{N}(t)$ as [43]

$${}_{t_0}I_t^\vartheta \mathcal{N}(t) = \frac{1}{\Gamma(\vartheta)} \int_{t_0}^t (t - \tau)^{\vartheta-1} \mathcal{N}(\tau) d\tau, \quad (1)$$

where $t \geq t_0$, $\vartheta > 0$, and $\Gamma(\vartheta) = \int_0^{+\infty} \tau^{\vartheta-1} e^{-\tau} d\tau$.

Definition 2. For a function $\mathcal{N}(t)$, define its Caputo derivative as [43]

$${}^c_{t_0}\mathcal{D}_t^\vartheta \mathcal{N}(t) = \frac{1}{\Gamma(\kappa - \vartheta)} \int_{t_0}^t (t - \tau)^{\kappa-\vartheta-1} \mathcal{N}^{(\kappa)}(\tau) d\tau, t \geq t_0, \quad (2)$$

where κ denotes a positive integer such that $0 \leq \kappa - 1 < \vartheta < \kappa$. Moreover, if $0 < \vartheta < 1$, ${}^c_{t_0}\mathcal{D}_t^\vartheta \mathcal{N}(t) = \frac{1}{\Gamma(1-\vartheta)} \int_{t_0}^t (t - \tau)^{-\vartheta} \mathcal{N}'(\tau) d\tau$; if $\vartheta = 1$, ${}^c_{t_0}\mathcal{D}_t^\vartheta \mathcal{N}(t)$ becomes the traditional operator.

Consider a class of CFUMNNs with fuzzy operators and transmission delay as below:

$$\begin{aligned} {}^c_{t_0}\mathcal{D}_t^\vartheta \phi_p(t) = & -(c_p + \Delta c_p(t))\phi_p(t) + \sum_{q=1}^m u_{pq}(\phi_p(t))f_q(\phi_q(t)) \\ & + \sum_{q=1}^m v_{pq}(\phi_p(t-\eta))f_q(\phi_q(t-\eta)) + \Phi_p(\phi(t)) + I_p, \end{aligned} \quad (3)$$

where

$$\Phi_p(\phi(t)) = \sum_{q=1}^m d_{pq}\xi_q + \bigwedge_{q=1}^m \rho_{pq}f_q(\phi_q(t-\eta)) + \bigvee_{q=1}^m \varrho_{pq}f_q(\phi_q(t-\eta)) + \bigwedge_{q=1}^m w_{pq}\xi_q + \bigvee_{q=1}^m \tilde{w}_{pq}\xi_q,$$

and

$$u_{pq}(\phi_p(t)) = \begin{cases} \dot{u}_{pq}, & |\phi_p(t)| > \overline{\Upsilon}_p, \\ \dot{u}_{pq}, & |\phi_p(t)| \leq \overline{\Upsilon}_p, \end{cases} \quad v_{pq}(\phi_p(t-\eta)) = \begin{cases} \dot{v}_{pq}, & |\phi_p(t-\eta)| > \overline{\Upsilon}_p, \\ \dot{v}_{pq}, & |\phi_p(t-\eta)| \leq \overline{\Upsilon}_p. \end{cases}$$

${}^c_{t_0} \mathcal{D}_t^\vartheta$ represents Caputo derivative with $0 < \vartheta < 1$, and $p \in \mathbb{N}_1^m = \{1, 2, \dots, m\}$. $\phi_p(t)$ represents the state of the p -th unit at instant t . \wedge and \vee represent the fuzzy AND and fuzzy OR operations. \lceil_p represents the switching jump. \dot{u}_{pq} , \dot{u}_{pq} , \dot{v}_{pq} , and \dot{v}_{pq} denote known constants regarding memristances. $u_{pq}(\phi_p(t))$ and $v_{pq}(\phi_p(t - \eta))$ denote memristive connection weights at different instants t and $t - \eta$, where η is the transmission delay. c_p is the self-feedback link weight. $\Delta c_p(t)$ represent the bounded parameter uncertainty, defined by $|\Delta c_p(t)| \leq \lceil_p$. d_{pq} is the fuzzy feed-forward template. ρ_{pq} and ϱ_{pq} signify fuzzy feedback MIN and MAX templates. w_{pq} and \tilde{w}_{pq} signify fuzzy feed-forward MIN and MAX templates. $f_q(\cdot)$ signify the network activation behaviors. I_p and ζ_p characterize the external input and the bias of neuron p .

For the sake of characterization, denote $u_{pq}^- = \min\{\dot{u}_{pq}, \dot{u}_{pq}\}$, $v_{pq}^- = \min\{\dot{v}_{pq}, \dot{v}_{pq}\}$, $u_{pq}^+ = \max\{\dot{u}_{pq}, \dot{u}_{pq}\}$, and $v_{pq}^+ = \max\{\dot{v}_{pq}, \dot{v}_{pq}\}$. Using the differential inclusion technique, there exist $u_{pq} \in co(u_{pq}(\phi_p(t))) = [u_{pq}^-, u_{pq}^+]$ and $v_{pq} \in co(v_{pq}(\phi_p(t - \eta))) = [v_{pq}^-, v_{pq}^+]$ such that

$${}^c_{t_0} \mathcal{D}_t^\vartheta \phi_p(t) = -(c_p + \Delta c_p(t))\phi_p(t) + \sum_{q=1}^m u_{pq} f_q(\phi_q(t)) + \sum_{q=1}^m v_{pq} f_q(\phi_q(t - \eta)) + \Phi_p(\phi(t)) + I_p. \quad (4)$$

The initial values of system (4) are $\phi_p(s) = \lceil_p^\phi(s)$, $s \in [t_0 - \eta, t_0]$. Take (4) as the master system, and the consequential slave system is described as

$${}^c_{t_0} \mathcal{D}_t^\vartheta \psi_p(t) = -(c_p + \Delta c_p(t))\psi_p(t) + \sum_{q=1}^m u_{pq} f_q(\psi_q(t)) + \sum_{q=1}^m v_{pq} f_q(\psi_q(t - \eta)) + \Phi_p(\psi(t)) + I_p + K_p(t), \quad (5)$$

where

$$\Phi_p(\psi(t)) = \sum_{q=1}^m d_{pq} \zeta_q + \bigwedge_{q=1}^m \rho_{pq} f_q(\psi_q(t - \eta)) + \bigvee_{q=1}^m \varrho_{pq} f_q(\psi_q(t - \eta)) + \bigwedge_{q=1}^m w_{pq} \zeta_q + \bigvee_{q=1}^m \tilde{w}_{pq} \zeta_q,$$

$p \in \mathbb{N}_1^m = \{1, 2, \dots, m\}$, and $K_p(t)$ denote the feedback control protocols. The remaining parameters of (5) have similar implications as system (4) and the initial values of network system (5) are $\psi_p(s) = \lceil_p^\psi(s)$, $s \in [t_0 - \eta, t_0]$.

Define the synchronization error of master-slave systems as $e_p(t) = \psi_p(t) - \phi_p(t)$, $p \in \mathbb{N}_1^m = \{1, 2, \dots, m\}$, and we can derive the below error equation

$$\begin{aligned} & {}^c_{t_0} \mathcal{D}_t^\vartheta e_p(t) \\ &= -(c_p + \Delta c_p(t))e_p(t) + \sum_{q=1}^m u_{pq} [f_q(\psi_q(t)) - f_q(\phi_q(t))] \\ &+ \sum_{q=1}^m v_{pq} [f_q(\psi_q(t - \eta)) - f_q(\phi_q(t - \eta))] + \bigwedge_{q=1}^m \rho_{pq} [f_q(\psi_q(t - \eta)) - f_q(\phi_q(t - \eta))] \\ &+ \bigvee_{q=1}^m \varrho_{pq} [f_q(\psi_q(t - \eta)) - f_q(\phi_q(t - \eta))] + K_p(t). \end{aligned} \quad (6)$$

Then, feedback control mechanisms for fuzzy master networks and fuzzy slave networks with uncertainties and delays can be seen in Figure 1.

Remark 1. Unlike the fractional-order MNN models in [30–37], this paper introduces two types of fuzzy operators that make our delayed model have both memristors and fuzzy features. In addition, nonlinear activation behaviors and uncertain links are considered for network modeling. In terms of the model's generalization, the fuzzy CFUMNNs proposed in this article can adapt to more complex environments than existing models in [30–37].

Remark 2. The synchronization problems for various kinds of integer-order MNNs have been extensively studied. In [22], the nonlocal synchronization of stochastic MNNs with impulsive delay

was studied. In [25], the synchronization and anti-synchronization of MNNs with unbounded proportional delays were considered. In [26], the global synchronization of multi-layer MNNs with various delays was investigated. Furthermore, the global synchronization conditions of nonlinear quaternion-valued MNNs with uncertainties were derived in [27]. However, the above control schemes and analyzed methods in [22,25–27] cannot be applied to our fractional-order model since Caputo-type MNNs considered in this article have non-locality and memristive.

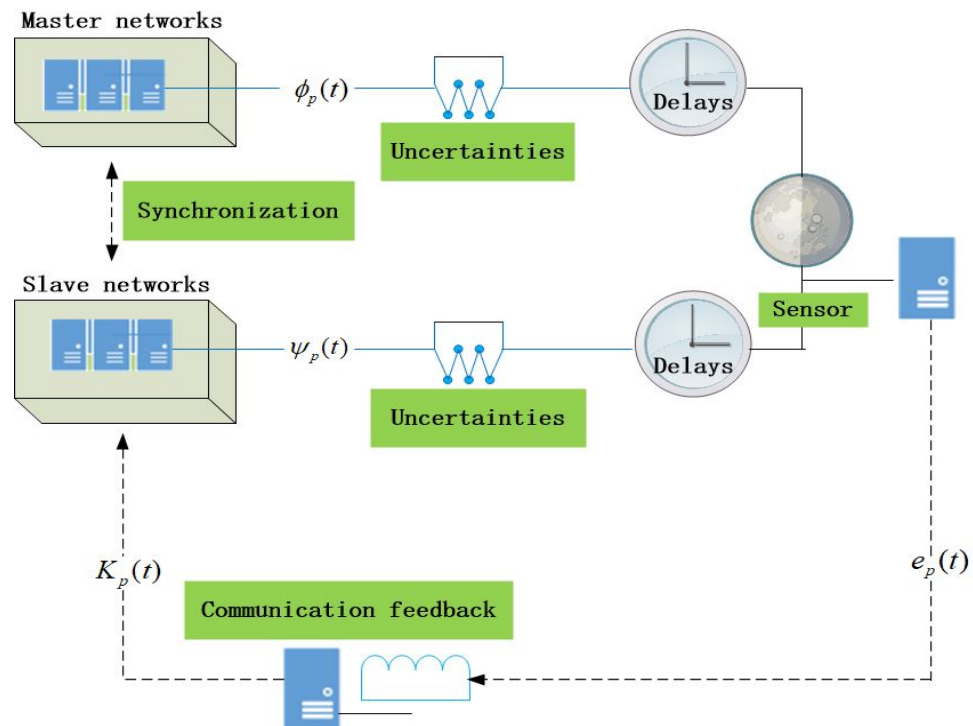


Figure 1. Feedback control mechanisms for fuzzy master networks and fuzzy slave networks with uncertainties and delays.

Definition 3. Fuzzy CFUMNNs (4) and (5) can achieved the FTS if there is an instant t^* making [44]

$$\lim_{t \rightarrow t^*} e_p(t) = 0 \text{ and } e_p(t) = 0, t > t^*, p \in \mathbb{N}_1^m, \quad (7)$$

where t^* represents the system settling time.

Lemma 1. Let $\rho_{pq}, q_{pq}, \psi_q(t - \eta), \phi_q(t - \eta) \in \mathbb{R}$ and $f_q : \mathbb{R} \rightarrow \mathbb{R}$ represent continuous functions. Then one can get [40]

$$\left| \bigwedge_{q=1}^m \rho_{pq} [f_q(\psi_q(t - \eta)) - f_q(\phi_q(t - \eta))] \right| \leq \sum_{q=1}^m |\rho_{pq}| |f_q(\psi_q(t - \eta)) - f_q(\phi_q(t - \eta))|, \quad (8)$$

and

$$\left| \bigvee_{q=1}^m q_{pq} [f_q(\psi_q(t - \eta)) - f_q(\phi_q(t - \eta))] \right| \leq \sum_{q=1}^m |q_{pq}| |f_q(\psi_q(t - \eta)) - f_q(\phi_q(t - \eta))|, \quad (9)$$

where $p, q \in \mathbb{N}_1^m$.

Assumption 1. Nonlinear functions $f_q : \mathbb{R} \rightarrow \mathbb{R}$ satisfy the Lipschitz condition, i.e., there exist positive scalars L_q such that

$$|f_q(\psi_q(t)) - f_q(\phi_q(t))| \leq L_q |\psi_q(t) - \phi_q(t)|, \quad (10)$$

for $\forall \psi_q(t), \phi_q(t) \in \mathbb{R}$, and $q \in \mathbb{N}_1^m$.

Lemma 2 ([45]). Let $\mathcal{V}(t) \in \mathbb{C}^1([t_0, +\infty), \mathbb{R})$ is differentiable, we get

$${}_t^c \mathcal{D}_t^\vartheta |\mathcal{V}(t)| \leq \text{sign}(\mathcal{V}(t)) {}_t^c \mathcal{D}_t^\vartheta \mathcal{V}(t), \quad 0 < \vartheta < 1. \quad (11)$$

Lemma 3. Let $W(t) \in \mathbb{C}^1([t_0, +\infty), \mathbb{R}^+)$ is differentiable and satisfies [44]

$${}_t^c \mathcal{D}_t^\vartheta W(t) \leq -bW^{-\alpha}(t) - aW^{-\beta}(t), \quad W(t) \in \mathbb{R}^+ / \{0\}, \quad (12)$$

where $0 < \vartheta < 1, b > 0, a > 0, \alpha \geq 0$, and $\alpha < \beta \leq 1 + 2\alpha$. Then one has $\lim_{t \rightarrow t^*} W(t) = 0$ and $W(t) = 0, t \geq t^*$, where

$$t^* \leq T = \left[\frac{\Gamma(1+\vartheta)}{a(1+\beta)2^{\frac{\beta-2\alpha-1}{1+\alpha}}} \left(\left(W^{1+\alpha}(t_0) + \left(\frac{a}{b}\right)^{\frac{1+\alpha}{\beta-\alpha}} \right)^{\frac{1+\beta}{1+\alpha}} - \left(\frac{a}{b}\right)^{\frac{1+\beta}{\beta-\alpha}} \right) \right]^{\frac{1}{\vartheta}} + t_0. \quad (13)$$

Lemma 4. Let $W(t) \in \mathbb{C}^1([t_0, +\infty), \mathbb{R}^+)$ is differentiable and satisfies [44]

$${}_t^c \mathcal{D}_t^\vartheta W(t) \leq -aW^{-\beta}(t) - b, \quad W(t) \in \mathbb{R}^+ / \{0\}, \quad (14)$$

where $0 < \vartheta < 1, b > 0, a > 0$, and $0 < \beta < 1$. Then one has $\lim_{t \rightarrow t^*} W(t) = 0$ and $W(t) = 0, t \geq t^*$, where

$$t^* \leq T = \left[\frac{\Gamma(1+\vartheta)}{a(1+\beta)2^{\beta-1}} \left(\left(W(t_0) + \left(\frac{a}{b}\right)^{\frac{1}{\beta}} \right)^{1+\beta} - \left(\frac{a}{b}\right)^{\frac{1+\beta}{\beta}} \right) \right]^{\frac{1}{\vartheta}} + t_0. \quad (15)$$

3. Novel Finite-Time Synchronization Requirements

To achieve the FTS tasks between master-slave systems (4) and (5), information feed-back control inputs are given by

$$K_p(t) = \begin{cases} -\gamma \frac{e_p(t)|e_p(t-\eta)|}{|e_p(t)|} - \delta e_p(t) - \epsilon \frac{e_p(t)}{|e_p(t)|^\sigma} - \zeta \frac{e_p(t)}{|e_p(t)|^\lambda}, & |e_p(t)| \neq 0, \\ 0, & |e_p(t)| = 0. \end{cases} \quad (16)$$

where $p \in \mathbb{N}_1^m$, and $\gamma, \delta, \epsilon, \zeta$ denote positive constants. $\sigma \geq 1$ and $\sigma < \lambda < 2\sigma$ represent tunable parameters.

Theorem 1. Under Assumption 1 and control protocol (16), CFUMNNs (4) are synchronized with CFUMNNs (5) in finite time if the below conditions

$$\delta \geq \max_{1 \leq p \leq m} \left[-c_p + \mathfrak{I}_p + \sum_{q=1}^m |u_{qp}| L_p \right] \quad (17)$$

and

$$\gamma \geq \max_{1 \leq p \leq m} \left[\sum_{q=1}^m (|v_{qp}| + |\rho_{qp}| + |\varrho_{qp}|) L_p \right] \quad (18)$$

hold. Furthermore, the settling time satisfies

$$t^* \leq t_1 = \left[\frac{\Gamma(1+\vartheta)}{m\zeta\lambda 2^{\frac{\lambda-2\sigma}{\sigma}}} \left(\left(W^\sigma(t_0) + \left(\frac{\zeta}{\epsilon}\right)^{\frac{\sigma}{\lambda-\sigma}} \right)^{\frac{\lambda}{\sigma}} - \left(\frac{\zeta}{\epsilon}\right)^{\frac{\lambda}{\lambda-\sigma}} \right) \right]^{\frac{1}{\vartheta}} + t_0. \quad (19)$$

Proof. Consider the auxiliary function

$$W(t) = \sum_{p=1}^m |e_p(t)|. \quad (20)$$

Based on Lemmas 1 and 2 and Equation (6), calculating the fractional derivative of $W(t)$ gives

$$\begin{aligned} & {}_{t_0}^c \mathcal{D}_t^\theta W(t) \\ & \leq \sum_{p=1}^m \text{sign}(e_p(t)) {}_{t_0}^c \mathcal{D}_t^\theta e_p(t) \\ & = \sum_{p=1}^m \text{sign}(e_p(t)) \left[-(c_p + \Delta c_p(t))e_p(t) + \sum_{q=1}^m u_{pq}[f_q(\psi_q(t)) - f_q(\phi_q(t))] \right. \\ & \quad + \sum_{q=1}^m v_{pq}[f_q(\psi_q(t-\eta)) - f_q(\phi_q(t-\eta))] + \sum_{q=1}^m \rho_{pq}[f_q(\psi_q(t-\eta)) - f_q(\phi_q(t-\eta))] \\ & \quad + \sum_{q=1}^m \varrho_{pq}[f_q(\psi_q(t-\eta)) - f_q(\phi_q(t-\eta))] - \gamma \frac{e_p(t)|e_p(t-\eta)|}{|e_p(t)|} \\ & \quad \left. - \delta e_p(t) - \epsilon \frac{e_p(t)}{|e_p(t)|^\sigma} - \zeta \frac{e_p(t)}{|e_p(t)|^\lambda} \right] \\ & \leq \sum_{p=1}^m \left[(-c_p + \beth_p)|e_p(t)| + \sum_{q=1}^m |u_{pq}|L_q|e_q(t)| + \sum_{q=1}^m |v_{pq}|L_q|e_q(t-\eta)| \right. \\ & \quad + \sum_{q=1}^m |\varrho_{pq}|L_q|e_q(t-\eta)| + \sum_{q=1}^m |\varrho_{pq}|L_q|e_q(t-\eta)| \\ & \quad \left. - \gamma|e_p(t-\eta)| - \delta|e_p(t)| - \epsilon|e_p(t)|^{1-\sigma} - \zeta|e_p(t)|^{1-\lambda} \right] \\ & = \sum_{p=1}^m \left[-c_p + \beth_p + \sum_{q=1}^m |u_{qp}|L_p - \delta \right] |e_p(t)| \\ & \quad + \sum_{p=1}^m \left[-\gamma + \sum_{q=1}^m (|v_{qp}| + |\rho_{qp}| + |\varrho_{qp}|)L_p \right] |e_p(t-\eta)| \\ & \quad - \sum_{p=1}^m \epsilon|e_p(t)|^{1-\sigma} - \sum_{p=1}^m \zeta|e_p(t)|^{1-\lambda}. \end{aligned} \quad (21)$$

Substituting (17) and (18) into (21), one can obtain

$${}_{t_0}^c \mathcal{D}_t^\theta W(t) \leq - \sum_{p=1}^m \epsilon|e_p(t)|^{1-\sigma} - \sum_{p=1}^m \zeta|e_p(t)|^{1-\lambda}. \quad (22)$$

For $\sigma \geq 1, m \in \mathbb{Z}^+$, it is not difficult to attain

$$\sum_{p=1}^m |e_p(t)|^{1-\sigma} \geq m \left(\sum_{p=1}^m |e_p(t)| \right)^{1-\sigma}. \quad (23)$$

Similarly, for $\sigma < \lambda < 2\sigma$ and $m \in \mathbb{Z}^+$, one can easily derive

$$\sum_{p=1}^m |e_p(t)|^{1-\lambda} \geq m \left(\sum_{p=1}^m |e_p(t)| \right)^{1-\lambda}. \quad (24)$$

Substituting (23) and (24) into (22), we can get

$$\begin{aligned} {}_{t_0}^c \mathcal{D}_t^\theta W(t) & \leq -m\epsilon \left(\sum_{p=1}^m |e_p(t)| \right)^{1-\sigma} - m\zeta \left(\sum_{p=1}^m |e_p(t)| \right)^{1-\lambda} \\ & \leq -m\epsilon W^{-(\sigma-1)}(t) - m\zeta W^{-(\lambda-1)}(t). \end{aligned} \quad (25)$$

Note that $m\epsilon > 0$, $m\zeta > 0$, $\sigma - 1 \geq 0$, $\lambda - 1 > 0$, and $\sigma - 1 < \lambda - 1 < 2\sigma - 1$. The coefficients of differential inequality (25) satisfy the framework requirements of Lemma 3. According to Lemma 3, CFUMNNs (4) are synchronized with CFUMNNs (5) in finite time under feedback controller (16) and the settling time satisfies

$$t^* \leq t_1 = \left[\frac{\Gamma(1+\vartheta)}{m\zeta\lambda 2^{\frac{\lambda-2\sigma}{\sigma}}} \left(\left(W^\sigma(t_0) + \left(\frac{\zeta}{\epsilon} \right)^{\frac{\sigma}{\lambda-\sigma}} \right)^{\frac{\lambda}{\sigma}} - \left(\frac{\zeta}{\epsilon} \right)^{\frac{\lambda}{\lambda-\sigma}} \right) \right]^{\frac{1}{\vartheta}} + t_0. \quad (26)$$

□

Remark 3. Different from the control protocols in [19–21], this article designs discontinuous information feedback control protocols consisting of three functional sub-modules to achieve the FTS target. In particular, $-\gamma \frac{e_p(t)|e_p(t-\eta)|}{|e_p(t)|}$ has the function of overcoming the time-delay interference; $-\delta e_p(t)$ has the effect of eliminating the quasi-linear growth error; $-\epsilon \frac{e_p(t)}{|e_p(t)|^\sigma} - \zeta \frac{e_p(t)}{|e_p(t)|^\lambda}$ has the role of implementing the synchronization task, where the control parameters ϵ and ζ affect the synchronization efficiency.

Remark 4. Evidently, the first equation in the information feedback protocols (16) shows that $\lim_{e_p(t) \rightarrow 0} K_p(t) = \infty$. In practical applications, a simple approach is to replace $-\gamma \frac{e_p(t)|e_p(t-\eta)|}{|e_p(t)|} - \delta e_p(t) - \epsilon \frac{e_p(t)}{|e_p(t)|^\sigma} - \zeta \frac{e_p(t)}{|e_p(t)|^\lambda}$ in (16) with $-\gamma \frac{e_p(t)|e_p(t-\eta)|}{|e_p(t)|+\epsilon} - \delta e_p(t) - \epsilon \frac{e_p(t)}{|e_p(t)|^{\sigma+\epsilon}} - \zeta \frac{e_p(t)}{|e_p(t)|^{\lambda+\epsilon}}$, where $\epsilon > 0$ denotes a small enough constant.

When control parameter $\sigma = 1$, the information feedback control input $K_p(t)$ can be adjusted as

$$K_p(t) = \begin{cases} -\gamma \frac{e_p(t)|e_p(t-\eta)|}{|e_p(t)|} - \delta e_p(t) - \epsilon \frac{e_p(t)}{|e_p(t)|} - \zeta \frac{e_p(t)}{|e_p(t)|^\lambda}, & |e_p(t)| \neq 0, \\ 0, & |e_p(t)| = 0. \end{cases} \quad (27)$$

where $p \in \mathbb{N}_1^m$, $\gamma, \delta, \epsilon, \zeta$ denote positive constants, and $1 < \lambda < 2$ represents a tunable parameter. Significantly, by constructing the Lyapunov function and utilizing a similar analysis for inequality (25), we can get

$${}_0^c \mathcal{D}_t^\vartheta W(t) \leq -m\epsilon - m\zeta W^{-(\lambda-1)}(t). \quad (28)$$

Then, using Lemma 4, one can derive the following Theorem 2.

Theorem 2. Under Assumption 1 and control protocol (27), CFUMNNs (4) are synchronized with CFUMNNs (5) in finite time if conditions (17) and (18) hold. Furthermore, the settling time satisfies

$$t^* \leq t_2 = \left[\frac{\Gamma(1+\vartheta)}{m\zeta\lambda 2^{\lambda-2}} \left(\left(W(t_0) + \left(\frac{\zeta}{\epsilon} \right)^{\frac{1}{\lambda-1}} \right)^\lambda - \left(\frac{\zeta}{\epsilon} \right)^{\frac{\lambda}{\lambda-1}} \right) \right]^{\frac{1}{\vartheta}} + t_0. \quad (29)$$

Remark 5. Based on inequalities (19) and (29), it is not difficult to evaluate the settling time t_1 and t_2 . Clearly, the settling time t_1 and t_2 rely on not only the degree ϑ , neuron number m , and the starting value $W(t_0)$, but also the control parameters ζ, ϵ , and λ . The only difference between the two inequalities is that there exists an additional control parameter σ in inequality (19), making it more generalizable.

Remark 6. It should be noted that the feedback control strategies and finite time synchronization results in this article are still applicable to integer-order fuzzy MNNs with transmission delays. The main reason is that the fractional-order lemmas utilized in this article can be directly extended

to integer-order ones. However, the comparison theorems and synchronization results in most integer-order NNs cannot be directly extended to fractional-order NNs.

Especially, if the parameter uncertainty is not considered for modeling networks, then CFUMNNs (4) representing the master system will be degenerated into

$${}^c_{t_0}\mathcal{D}_t^\vartheta \phi_p(t) = -c_p \phi_p(t) + \sum_{q=1}^m u_{pq} f_q(\phi_q(t)) + \sum_{q=1}^m v_{pq} f_q(\phi_q(t - \eta)) + \Phi_p(\phi(t)) + I_p. \quad (30)$$

Correspondingly, CFUMNNs (5) representing the slave system will be degenerated into

$${}^c_{t_0}\mathcal{D}_t^\vartheta \psi_p(t) = -c_p \psi_p(t) + \sum_{q=1}^m u_{pq} f_q(\psi_q(t)) + \sum_{q=1}^m v_{pq} f_q(\psi_q(t - \eta)) + \Phi_p(\psi(t)) + I_p + K_p(t). \quad (31)$$

Based on the synchronization criteria in Theorems 1 and 2, one gets the below monumental corollaries.

Corollary 1. Under Assumption 1 and control protocol (16), CFUMNNs (30) are synchronized with CFUMNNs (31) in finite time if the below conditions

$$\delta \geq \max_{1 \leq p \leq m} \left[-c_p + \sum_{q=1}^m |u_{qp}| L_p \right] \quad (32)$$

and

$$\gamma \geq \max_{1 \leq p \leq m} \left[\sum_{q=1}^m (|v_{qp}| + |\rho_{qp}| + |\varrho_{qp}|) L_p \right] \quad (33)$$

hold. Furthermore, the settling time satisfies

$$t^* \leq t_3 = \left[\frac{\Gamma(1 + \vartheta)}{m\zeta\lambda 2^{\frac{\lambda-2\vartheta}{\sigma}}} \left(\left(W^\sigma(t_0) + \left(\frac{\zeta}{\epsilon} \right)^{\frac{\sigma}{\lambda-\sigma}} \right)^{\frac{\lambda}{\sigma}} - \left(\frac{\zeta}{\epsilon} \right)^{\frac{\lambda}{\lambda-\sigma}} \right) \right]^{\frac{1}{\vartheta}} + t_0. \quad (34)$$

Corollary 2. Under Assumption 1 and control protocol (27), CFUMNNs (30) are synchronized with CFUMNNs (31) in finite time if conditions (32) and (33) hold. Furthermore, the settling time satisfies

$$t^* \leq t_4 = \left[\frac{\Gamma(1 + \vartheta)}{m\zeta\lambda 2^{\lambda-2}} \left(\left(W(t_0) + \left(\frac{\zeta}{\epsilon} \right)^{\frac{1}{\lambda-1}} \right)^\lambda - \left(\frac{\zeta}{\epsilon} \right)^{\frac{\lambda}{\lambda-1}} \right) \right]^{\frac{1}{\vartheta}} + t_0. \quad (35)$$

4. Verification Experiments

To illustrate the applicability of the principal FTS results derived in this study, two verification examples are constructed below.

Example 1. Take the following fractional-order uncertain MNNs with fuzzy operators and transmission delay as the drive system:

$$\begin{aligned} {}^c_{t_0}\mathcal{D}_t^{0.95} \phi_p(t) = & -(c_p + \Delta c_p(t)) \phi_p(t) + \sum_{q=1}^3 u_{pq} f_q(\phi_q(t)) + \sum_{q=1}^3 v_{pq} f_q(\phi_q(t - \eta)) \\ & + \Phi_p(\phi(t)) + I_p, \end{aligned} \quad (36)$$

where $\eta = 0.08$, $c_p = 1$, $\Delta c_p(t) = 0.1 \sin t$, $d_{pq} = -1$, $I_p = 0$, $w_{pp} = \tilde{w}_{pp} = -0.1$, $w_{pq} = \tilde{w}_{pq} = 0.1$ ($p \neq q$), $\rho_{11} = \rho_{13} = \rho_{22} = \rho_{23} = \rho_{31} = \rho_{32} = \varrho_{23} = \varrho_{32} = 0.1$, $\rho_{12} = \rho_{21} = \varrho_{12} = \varrho_{21} = -0.2$, $\rho_{33} = \varrho_{33} = -0.1$, $\varrho_{11} = \varrho_{13} = \varrho_{22} = \varrho_{31} = 0.2$, and the memristive connection weights are defined as

$$\begin{aligned}
u_{11}(\phi_1) &= \begin{cases} 2.0, & |\phi_1(t)| > 1, \\ 2.2, & |\phi_1(t)| \leq 1, \end{cases} & u_{12}(\phi_1) &= \begin{cases} -1.0, & |\phi_1(t)| > 1, \\ -1.2, & |\phi_1(t)| \leq 1, \end{cases} \\
u_{13}(\phi_1) &= \begin{cases} 1.8, & |\phi_1(t)| > 1, \\ 2.0, & |\phi_1(t)| \leq 1, \end{cases} & u_{21}(\phi_2) &= \begin{cases} 0.8, & |\phi_2(t)| > 1, \\ 1.0, & |\phi_2(t)| \leq 1, \end{cases} \\
u_{22}(\phi_2) &= \begin{cases} 1.5, & |\phi_2(t)| > 1, \\ 1.8, & |\phi_2(t)| \leq 1, \end{cases} & u_{23}(\phi_2) &= \begin{cases} -1.0, & |\phi_2(t)| > 1, \\ -1.5, & |\phi_2(t)| \leq 1, \end{cases} \\
u_{31}(\phi_3) &= \begin{cases} -1.1, & |\phi_3(t)| > 1, \\ -1.0, & |\phi_3(t)| \leq 1, \end{cases} & u_{32}(\phi_3) &= \begin{cases} 2.0, & |\phi_3(t)| > 1, \\ 1.7, & |\phi_3(t)| \leq 1, \end{cases} \\
u_{33}(\phi_3) &= \begin{cases} 1.5, & |\phi_3(t)| > 1, \\ 2.0, & |\phi_3(t)| \leq 1, \end{cases} & v_{11}(\phi_1) &= \begin{cases} -2.0, & |\phi_1(t)| > 1, \\ -1.5, & |\phi_1(t)| \leq 1, \end{cases} \\
v_{12}(\phi_1) &= \begin{cases} -0.5, & |\phi_1(t)| > 1, \\ -1.0, & |\phi_1(t)| \leq 1, \end{cases} & v_{13}(\phi_1) &= \begin{cases} 1.5, & |\phi_1(t)| > 1, \\ 2.0, & |\phi_1(t)| \leq 1, \end{cases} \\
v_{21}(\phi_2) &= \begin{cases} 2.5, & |\phi_2(t)| > 1, \\ 2.2, & |\phi_2(t)| \leq 1, \end{cases} & v_{22}(\phi_2) &= \begin{cases} 5.0, & |\phi_2(t)| > 1, \\ 4.5, & |\phi_2(t)| \leq 1, \end{cases} \\
v_{23}(\phi_2) &= \begin{cases} -2.5, & |\phi_2(t)| > 1, \\ -3.0, & |\phi_2(t)| \leq 1, \end{cases} & v_{31}(\phi_3) &= \begin{cases} 2.4, & |\phi_3(t)| > 1, \\ 2.0, & |\phi_3(t)| \leq 1, \end{cases} \\
v_{32}(\phi_3) &= \begin{cases} -2.0, & |\phi_3(t)| > 1, \\ -1.8, & |\phi_3(t)| \leq 1, \end{cases} & v_{33}(\phi_3) &= \begin{cases} 4.5, & |\phi_3(t)| > 1, \\ 5.0, & |\phi_3(t)| \leq 1, \end{cases}
\end{aligned}$$

Let the activation functions $f_q(\phi_q(t)) = \tanh(|\phi_q(t)| - 1)$. Through simple calculations, one derives that $L_1 = L_2 = L_3 = 1$ satisfies Assumption 1. Based on drive system (36), one can obtain the response system as

$$\begin{aligned}
{}^c_{t_0} \mathcal{D}_t^{0.95} \psi_p(t) = & -(c_p + \Delta c_p(t)) \psi_p(t) + \sum_{q=1}^3 u_{pq} f_q(\psi_q(t)) + \sum_{q=1}^3 v_{pq} f_q(\psi_q(t - \eta)) \\
& + \Phi_p(\psi(t)) + I_p + K_p(t),
\end{aligned} \quad (37)$$

where

$$\begin{aligned}
u_{11}(\psi_1) &= \begin{cases} 2.0, & |\psi_1(t)| > 1, \\ 2.2, & |\psi_1(t)| \leq 1, \end{cases} & u_{12}(\psi_1) &= \begin{cases} -1.0, & |\psi_1(t)| > 1, \\ -1.2, & |\psi_1(t)| \leq 1, \end{cases} \\
u_{13}(\psi_1) &= \begin{cases} 1.8, & |\psi_1(t)| > 1, \\ 2.0, & |\psi_1(t)| \leq 1, \end{cases} & u_{21}(\psi_2) &= \begin{cases} 0.8, & |\psi_2(t)| > 1, \\ 1.0, & |\psi_2(t)| \leq 1, \end{cases} \\
u_{22}(\psi_2) &= \begin{cases} 1.5, & |\psi_2(t)| > 1, \\ 1.8, & |\psi_2(t)| \leq 1, \end{cases} & u_{23}(\psi_2) &= \begin{cases} -1.0, & |\psi_2(t)| > 1, \\ -1.5, & |\psi_2(t)| \leq 1, \end{cases} \\
u_{31}(\psi_3) &= \begin{cases} -1.1, & |\psi_3(t)| > 1, \\ -1.0, & |\psi_3(t)| \leq 1, \end{cases} & u_{32}(\psi_3) &= \begin{cases} 2.0, & |\psi_3(t)| > 1, \\ 1.7, & |\psi_3(t)| \leq 1, \end{cases} \\
u_{33}(\psi_3) &= \begin{cases} 1.5, & |\psi_3(t)| > 1, \\ 2.0, & |\psi_3(t)| \leq 1, \end{cases} & v_{11}(\psi_1) &= \begin{cases} -2.0, & |\psi_1(t)| > 1, \\ -1.5, & |\psi_1(t)| \leq 1, \end{cases} \\
v_{12}(\psi_1) &= \begin{cases} -0.5, & |\psi_1(t)| > 1, \\ -1.0, & |\psi_1(t)| \leq 1, \end{cases} & v_{13}(\psi_1) &= \begin{cases} 1.5, & |\psi_1(t)| > 1, \\ 2.0, & |\psi_1(t)| \leq 1, \end{cases} \\
v_{21}(\psi_2) &= \begin{cases} 2.5, & |\psi_2(t)| > 1, \\ 2.2, & |\psi_2(t)| \leq 1, \end{cases} & v_{22}(\psi_2) &= \begin{cases} 5.0, & |\psi_2(t)| > 1, \\ 4.5, & |\psi_2(t)| \leq 1, \end{cases}
\end{aligned}$$

$$v_{23}(\psi_2) = \begin{cases} -2.5, & |\psi_2(t)| > 1, \\ -3.0, & |\psi_2(t)| \leq 1, \end{cases} \quad v_{31}(\psi_3) = \begin{cases} 2.4, & |\psi_3(t)| > 1, \\ 2.0, & |\psi_3(t)| \leq 1, \end{cases}$$

$$v_{32}(\psi_3) = \begin{cases} -2.0, & |\psi_3(t)| > 1, \\ -1.8, & |\psi_3(t)| \leq 1, \end{cases} \quad v_{33}(\psi_3) = \begin{cases} 4.5, & |\psi_3(t)| > 1, \\ 5.0, & |\psi_3(t)| \leq 1, \end{cases}$$

and other network parameters have similar forms as network (36).

Let control parameters in response system (37) as $\gamma = 11.5$, $\delta = 5.5$, $\epsilon = 0.2$, $\zeta = 0.2$, $\sigma = 1.1$, $\lambda = 1.2$. Uncomplicated calculations yield that $\delta - \max_{1 \leq p \leq m} \left[-c_p + \mathfrak{I}_p + \sum_{q=1}^m |u_{qp}| L_p \right] > 0.9$, and $\gamma - \max_{1 \leq p \leq m} \left[\sum_{q=1}^m (|v_{qp}| + |\rho_{qp}| + |\varrho_{qp}|) L_p \right] > 0.8$, which satisfies the synchronization constraints of Theorem 1.

To test the robustness of the results in this article, the starting values for the neural states of fuzzy CFUMNNs (36) and (37) are randomly produced in $[-1, 1]$ and prediction correction methods have been utilized for experiment simulations. Under the above system parameters and control strengths, the evolution trajectories of drive-response systems (36) and (37) gradually overlap, as shown in the first three subgraphs in Figure 2. Meanwhile, the synchronization errors between systems (36) and (37) asymptotically converge to zero, as shown in Figure 2d–f. Hence, the synchronization objective can be achieved in finite time $t^* \leq 5.3372$ and the effectiveness of Theorem 1 has been validated. To discuss the influence of different parameters on the derived results, we define the overall system error as $E(t) = \sum_{p=1}^m |e_p(t)|$. First, maintain the same control intensity and regulate the size of the transmission delay with an initialization of 0.10 and a step of 0.04, it can be concluded that the greater the delay, the longer the control time for the system to achieve synchronization, as illustrated in Figure 3a. Second, the uncertainties are adjusted to 0.20sint, 0.40sint, and 0.60sint, respectively. One can easily find that the greater the magnitude of the uncertainty function, the more difficult to achieve the FTS objective. To further investigate the effect of fractional order on the synchronization results. We adjusted the fractional order to 0.7, 0.8 and 1.0, and the experimental results in Figure 4 showed that the synchronization results in this paper are still valid.

Remark 7. Due to the non-local nature of fractional neural networks, a prediction correction technique named Adams-Bashforth-Moulton [46] is applied in numerical simulations of Matlab R2020b to solve delayed fractional order differential equations. The whole solution process contains two main phases: prediction and correction. Firstly, a grid method is used to delimit the time interval. A product rectangle rule is used to evaluate the prediction term, and a product trapezoidal summation rule is employed to obtain the correction formulators. Based on two important rules, the numerical solution is easily implemented.

Example 2. Consider the below fractional-order uncertain delayed MNNs with fuzzy operators as the drive system:

$${}^c_{t_0} \mathcal{D}_t^{0.92} \phi_p(t) = -(c_p + \Delta c_p(t)) \phi_p(t) + \sum_{q=1}^3 u_{pq} f_q(\phi_q(t)) + \sum_{q=1}^3 v_{pq} f_q(\phi_q(t - \eta)) + \Phi_p(\phi(t)) + I_p, \quad (38)$$

where $\eta = 0.10$, $c_p = 1$, $\Delta c_p(t) = 0.1 \cos t$, $d_{pq} = 1$, $I_p = 0$, $w_{pq} = \bar{w}_{pq} = 0.1$, $\rho_{11} = \rho_{13} = \rho_{22} = \rho_{23} = \rho_{31} = \rho_{32} = 0.1$, $\rho_{12} = \rho_{21} = -0.2$, $\rho_{33} = -0.1$, $\varrho_{11} = \varrho_{13} = \varrho_{22} = \varrho_{31} = 0.2$, $\varrho_{12} = \varrho_{21} = -0.2$, $\varrho_{23} = \varrho_{32} = 0.1$, $\varrho_{33} = -0.1$ and the memristive connection weights are selected as

$$u_{11}(\phi_1) = \begin{cases} 2.1, & |\phi_1(t)| > 1, \\ 2.0, & |\phi_1(t)| \leq 1, \end{cases} \quad u_{12}(\phi_1) = \begin{cases} -1.0, & |\phi_1(t)| > 1, \\ -1.1, & |\phi_1(t)| \leq 1, \end{cases}$$

$$\begin{aligned}
u_{13}(\phi_1) &= \begin{cases} 1.8, & |\phi_1(t)| > 1, \\ 2.1, & |\phi_1(t)| \leq 1, \end{cases} & u_{21}(\phi_2) &= \begin{cases} 0.8, & |\phi_2(t)| > 1, \\ 1.1, & |\phi_2(t)| \leq 1, \end{cases} \\
u_{22}(\phi_2) &= \begin{cases} 1.5, & |\phi_2(t)| > 1, \\ 1.8, & |\phi_2(t)| \leq 1, \end{cases} & u_{23}(\phi_2) &= \begin{cases} -1.0, & |\phi_2(t)| > 1, \\ -1.3, & |\phi_2(t)| \leq 1, \end{cases} \\
u_{31}(\phi_3) &= \begin{cases} -1.1, & |\phi_3(t)| > 1, \\ -1.2, & |\phi_3(t)| \leq 1, \end{cases} & u_{32}(\phi_3) &= \begin{cases} 2.1, & |\phi_3(t)| > 1, \\ 1.7, & |\phi_3(t)| \leq 1, \end{cases} \\
u_{33}(\phi_3) &= \begin{cases} 1.5, & |\phi_3(t)| > 1, \\ 2.1, & |\phi_3(t)| \leq 1, \end{cases} & v_{11}(\phi_1) &= \begin{cases} -2.1, & |\phi_1(t)| > 1, \\ -1.8, & |\phi_1(t)| \leq 1, \end{cases} \\
v_{12}(\phi_1) &= \begin{cases} -0.5, & |\phi_1(t)| > 1, \\ -1.1, & |\phi_1(t)| \leq 1, \end{cases} & v_{13}(\phi_1) &= \begin{cases} 1.8, & |\phi_1(t)| > 1, \\ 2.1, & |\phi_1(t)| \leq 1, \end{cases} \\
v_{21}(\phi_2) &= \begin{cases} 2.5, & |\phi_2(t)| > 1, \\ 2.2, & |\phi_2(t)| \leq 1, \end{cases} & v_{22}(\phi_2) &= \begin{cases} 5.1, & |\phi_2(t)| > 1, \\ 4.5, & |\phi_2(t)| \leq 1, \end{cases} \\
v_{23}(\phi_2) &= \begin{cases} -2.5, & |\phi_2(t)| > 1, \\ -3.1, & |\phi_2(t)| \leq 1, \end{cases} & v_{31}(\phi_3) &= \begin{cases} 2.4, & |\phi_3(t)| > 1, \\ 2.1, & |\phi_3(t)| \leq 1, \end{cases} \\
v_{32}(\phi_3) &= \begin{cases} -2.1, & |\phi_3(t)| > 1, \\ -1.8, & |\phi_3(t)| \leq 1, \end{cases} & v_{33}(\phi_3) &= \begin{cases} 4.5, & |\phi_3(t)| > 1, \\ 5.1, & |\phi_3(t)| \leq 1, \end{cases}
\end{aligned}$$

Let the activation functions $f_q(\phi_q(t)) = \tanh(|\phi_q(t)| - 1)$. Clearly, $L_1 = L_2 = L_3 = 1$ satisfies Assumption 1. Based on drive system (38), one can obtain the response system as

$$\begin{aligned}
{}^c_{t_0} \mathcal{D}_t^{0.92} \psi_p(t) = & -(c_p + \Delta c_p(t)) \psi_p(t) + \sum_{q=1}^3 u_{pq} f_q(\psi_q(t)) + \sum_{q=1}^3 v_{pq} f_q(\psi_q(t - \eta)) \\
& + \Phi_p(\psi(t)) + I_p + K_p(t),
\end{aligned} \quad (39)$$

where

$$\begin{aligned}
u_{11}(\psi_1) &= \begin{cases} 2.1, & |\psi_1(t)| > 1, \\ 2.0, & |\psi_1(t)| \leq 1, \end{cases} & u_{12}(\psi_1) &= \begin{cases} -1.0, & |\psi_1(t)| > 1, \\ -1.1, & |\psi_1(t)| \leq 1, \end{cases} \\
u_{13}(\psi_1) &= \begin{cases} 1.8, & |\psi_1(t)| > 1, \\ 2.1, & |\psi_1(t)| \leq 1, \end{cases} & u_{21}(\psi_2) &= \begin{cases} 0.8, & |\psi_2(t)| > 1, \\ 1.1, & |\psi_2(t)| \leq 1, \end{cases} \\
u_{22}(\psi_2) &= \begin{cases} 1.5, & |\psi_2(t)| > 1, \\ 1.8, & |\psi_2(t)| \leq 1, \end{cases} & u_{23}(\psi_2) &= \begin{cases} -1.0, & |\psi_2(t)| > 1, \\ -1.3, & |\psi_2(t)| \leq 1, \end{cases} \\
u_{31}(\psi_3) &= \begin{cases} -1.1, & |\psi_3(t)| > 1, \\ -1.2, & |\psi_3(t)| \leq 1, \end{cases} & u_{32}(\psi_3) &= \begin{cases} 2.1, & |\psi_3(t)| > 1, \\ 1.7, & |\psi_3(t)| \leq 1, \end{cases} \\
u_{33}(\psi_3) &= \begin{cases} 1.5, & |\psi_3(t)| > 1, \\ 2.1, & |\psi_3(t)| \leq 1, \end{cases} & v_{11}(\psi_1) &= \begin{cases} -2.1, & |\psi_1(t)| > 1, \\ -1.8, & |\psi_1(t)| \leq 1, \end{cases} \\
v_{12}(\psi_1) &= \begin{cases} -0.5, & |\psi_1(t)| > 1, \\ -1.1, & |\psi_1(t)| \leq 1, \end{cases} & v_{13}(\psi_1) &= \begin{cases} 1.8, & |\psi_1(t)| > 1, \\ 2.1, & |\psi_1(t)| \leq 1, \end{cases} \\
v_{21}(\psi_2) &= \begin{cases} 2.5, & |\psi_2(t)| > 1, \\ 2.2, & |\psi_2(t)| \leq 1, \end{cases} & v_{22}(\psi_2) &= \begin{cases} 5.1, & |\psi_2(t)| > 1, \\ 4.5, & |\psi_2(t)| \leq 1, \end{cases} \\
v_{23}(\psi_2) &= \begin{cases} -2.5, & |\psi_2(t)| > 1, \\ -3.1, & |\psi_2(t)| \leq 1, \end{cases} & v_{31}(\psi_3) &= \begin{cases} 2.4, & |\psi_3(t)| > 1, \\ 2.1, & |\psi_3(t)| \leq 1, \end{cases}
\end{aligned}$$

$$v_{32}(\psi_3) = \begin{cases} -2.1, & |\psi_3(t)| > 1, \\ -1.8, & |\psi_3(t)| \leq 1, \end{cases} \quad v_{33}(\psi_3) = \begin{cases} 4.5, & |\psi_3(t)| > 1, \\ 5.1, & |\psi_3(t)| \leq 1. \end{cases}$$

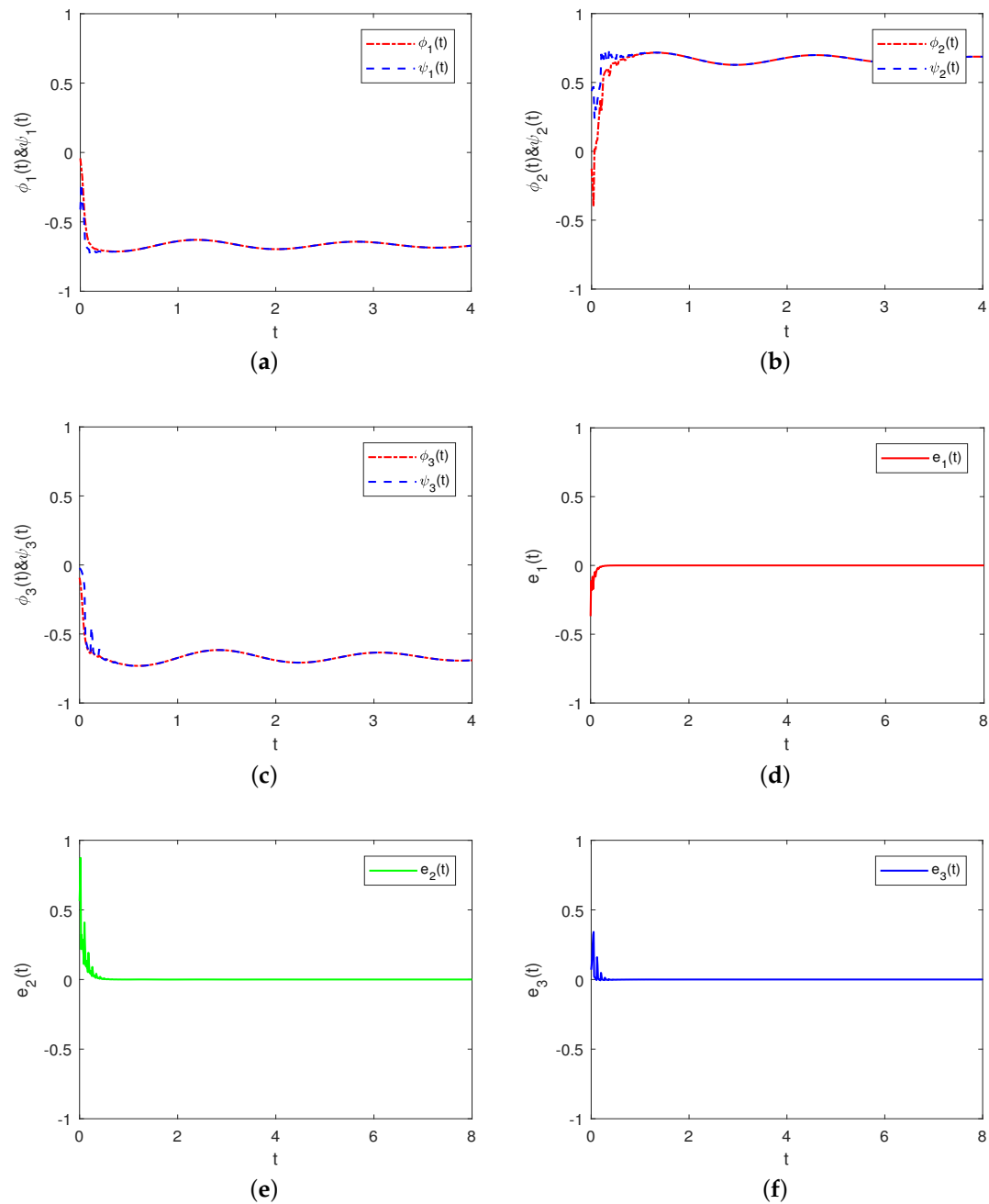


Figure 2. The evolution curves of state and error vectors for fuzzy CFUMNNs (36) and (37) under information feedback (16) in Example 1. (a) $\phi_1(t)$ & $\psi_1(t)$; (b) $\phi_2(t)$ & $\psi_2(t)$; (c) $\phi_3(t)$ & $\psi_3(t)$; (d) $e_1(t)$; (e) $e_2(t)$; (f) $e_3(t)$.

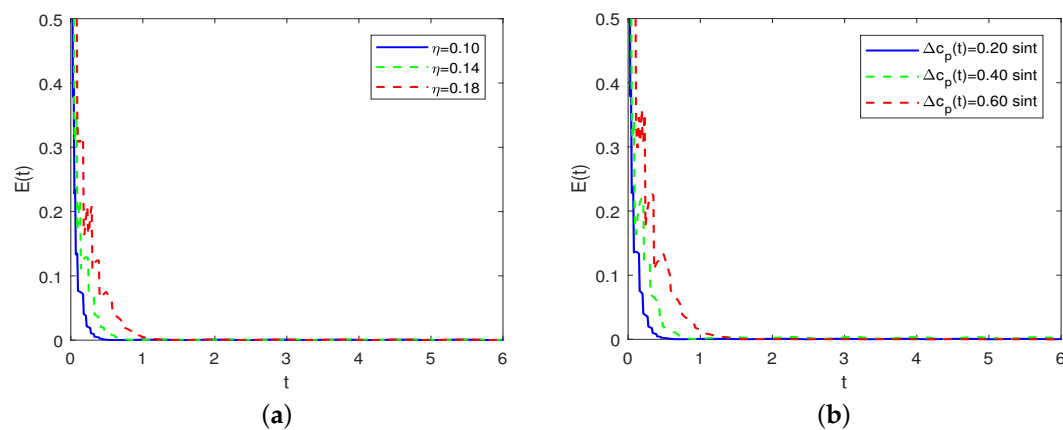


Figure 3. The overall system error $E(t)$ between fuzzy CFUMNNs (36) and (37) under information feedback (16) with adjusted parameters in Example 1. (a) $E(t)$ under different transmission delays; (b) $E(t)$ under different uncertain links.

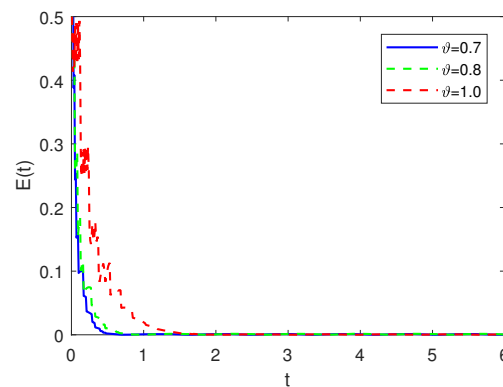


Figure 4. The overall system error $E(t)$ between fuzzy CFUMNNs (36) and (37) under information feedback (16) with different fractional order in Example 1.

Let control parameters in response system (39) as $\gamma = 11.6, \delta = 5.4, \epsilon = 0.2, \zeta = 0.2, \lambda = 1.2$. Simple calculations give that $\delta - \max_{1 \leq p \leq m} \left[-c_p + \mathfrak{I}_p + \sum_{q=1}^m |u_{qp}| L_p \right] > 0.8$, and $\gamma - \max_{1 \leq p \leq m} \left[\sum_{q=1}^m (|v_{qp}| + |\rho_{qp}| + |\varrho_{qp}|) L_p \right] > 0.6$, which implies the synchronization constraints of Theorem 2 hold.

To achieve the FTS objective, information feedback control protocol (27) is applied for fuzzy CFUMNNs (38) and (39), and the initial values for the neural states are also randomly produced in $[-1, 1]$. As illustrated in Figure 5, the time evolution of state variables and error variables indicates that the FTS can be achieved between drive-response systems (38) and (39) under control protocol (27) with suitable parameters. Meanwhile, the finite time measurement can be obtained as $t^* \leq 5.5354$. To verify the robustness of the control strategy to different parameters, we maintain the same control intensity and regulate the size of the transmission delay with an initialization 0.15 and a step 0.05, one can conclude that the greater the delay, the longer the evolution time to reach synchronization, as illustrated in Figure 6a. Moreover, changing the uncertainties as 0.20cost, 0.40cost, and 0.60cost, as illustrated in Figure 6b, we can readily derive that the greater the magnitude of the uncertainty function, the more difficult to achieve the synchronization goal. Both examples in this section demonstrate that transmission delays and uncertainties affect the stability of error systems and the synchronization efficiency of drive-response networks.

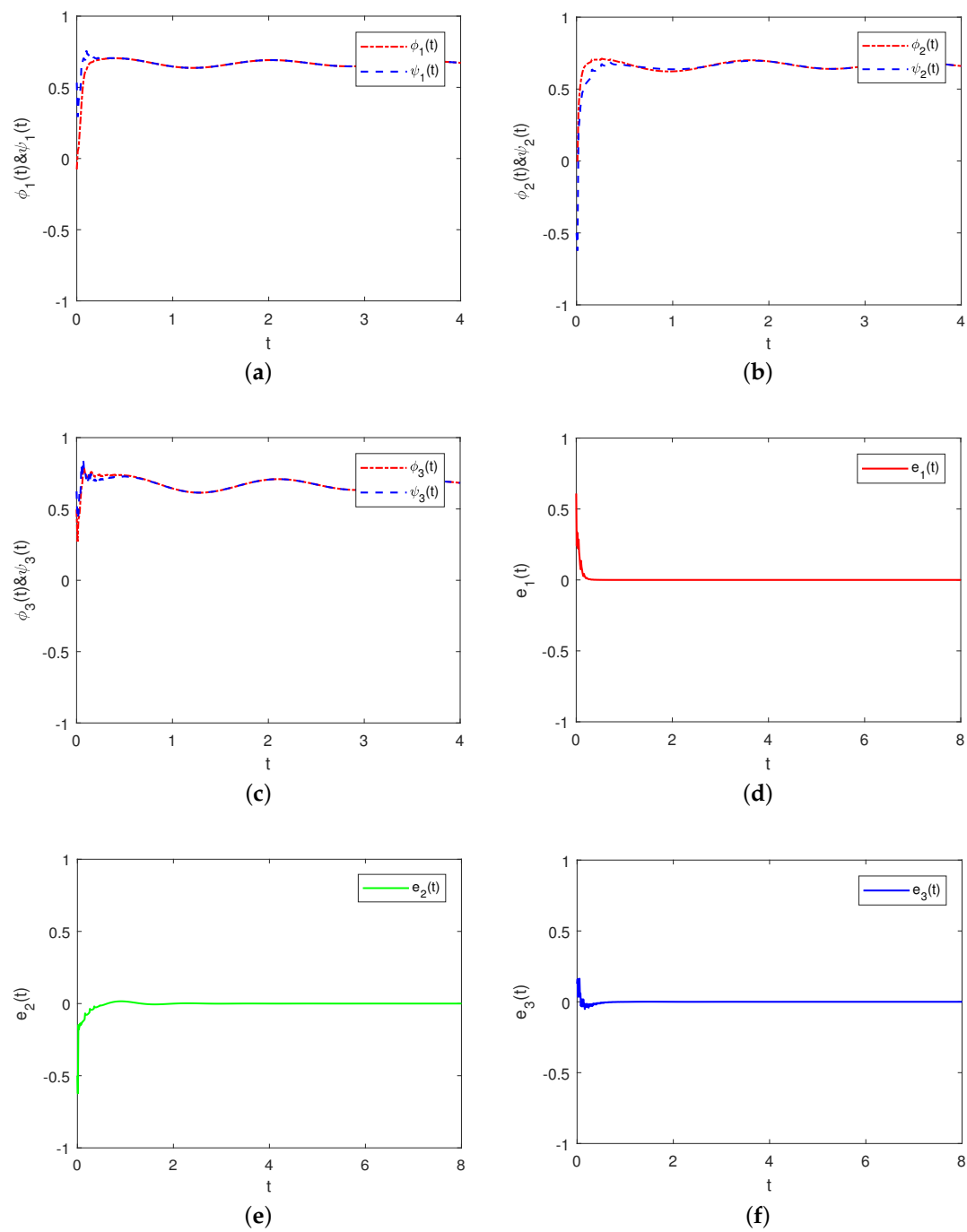


Figure 5. The curves of state and error vectors for fuzzy CFUMNNs (38) and (39) under information feedback (27) in Example 2. (a) $\phi_1(t)$ & $\psi_1(t)$; (b) $\phi_2(t)$ & $\psi_2(t)$; (c) $\phi_3(t)$ & $\psi_3(t)$; (d) $e_1(t)$; (e) $e_2(t)$; (f) $e_3(t)$.

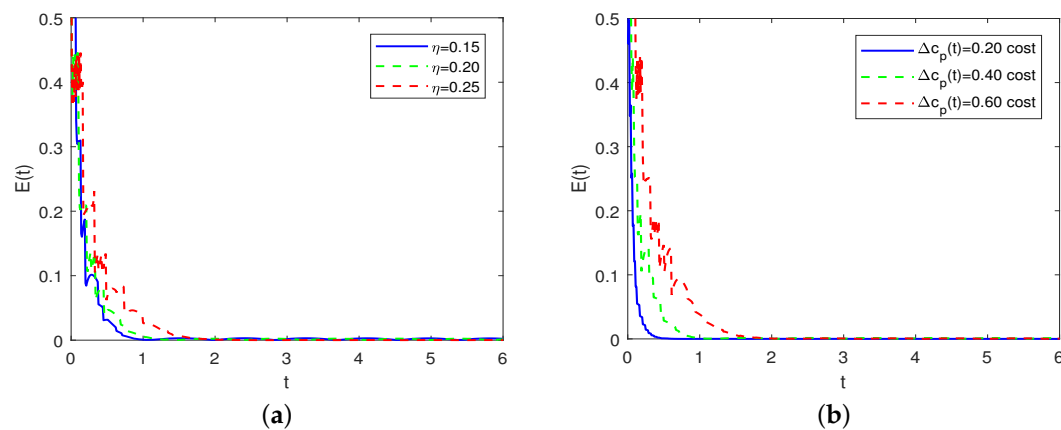


Figure 6. The overall system error $E(t)$ between fuzzy CFUMNNs (38) and (39) under information feedback (27) with adjusted parameters in Example 2. (a) $E(t)$ under different transmission delays; (b) $E(t)$ under different uncertain links.

5. Conclusions

The research in this article focuses on the finite-time synchronization challenge for fractional-order uncertain MNNs with transmission delay. In particular, two kinds of fuzzy operators and nonlinear activation behaviors are introduced into the generalized master-slave systems. It becomes a challenging task to design a suitable controller to overcome the multiple factors in the networks. We have considered a composite control protocol consisting of three parts to eliminate the quasi-linear growth error, overcome the time-delay effect, and implement the synchronization tasks. Using the comparative theorem and Lyapunov function approach, novel delay-independent synchronization criteria have been presented in the form of inequalities. Furthermore, the estimation of the settling time boundary and the impact of major factors on synchronization results have also been studied. In future research, additional optimization studies of intermittent feedback control techniques based on event-triggering mechanisms are necessary to reduce the control burden and enhance information safety.

Author Contributions: Conceptualization, K.S., H.F. and Z.G.; Methodology, K.S. and Z.G.; Software, H.F. and A.Z.; Writing—original draft, H.F., K.S. and A.Z.; Writing—review and editing, H.F., K.S. and Z.G. All authors have read and agreed to the published version of the manuscript.

Funding: The first author was partially supported by the Open Foundation of Engineering Research Center of Big Data Application in Private Health Medicine, Fujian Province University under Grant (MKF202201), and the APC was funded by (MKF202201). The second author was partially supported by the Sichuan Science and Technology Program under Grant (21YYJC0469), and the Key R&D Projects of Sichuan Provincial Department of Science and Technology under Grant (2023YFG0287).

Data Availability Statement: Data is contained within the article.

Conflicts of Interest: The authors declare no conflict of interest.

References

1. Dou, H.; Shen, F.; Zhao, J.; Mu, X.Y. Understanding neural network through neuron level visualization. *Neural Netw.* **2023**, *168*, 484–495. [[CrossRef](#)] [[PubMed](#)]
2. Navarin, N.; Mulders, D.; Oneto, L. Advances in artificial neural networks. machine learning and computational intelligence. *Neurocomputing* **2024**, *571*, 127098. [[CrossRef](#)]
3. Tang, Z.; Xuan, D.L.; Park, J.H.; Wang, Y.; Feng, J.W. Impulsive effects based distributed synchronization of heterogeneous coupled neural networks. *IEEE Trans. Netw. Sci. Eng.* **2021**, *8*, 498–510. [[CrossRef](#)]
4. Ding, K.; Zhu, Q.X. A note on sampled-data synchronization of memristor networks subject to actuator failures and two different activations. *IEEE Trans. Circuits Syst. II Express Briefs* **2021**, *68*, 2097–2101. [[CrossRef](#)]

5. Cai, J.Y.; Yi, C.B.; Wu, Y.; Liu, D.Q.; Zhong, D.G. Leader-following consensus of nonlinear singular switched multi-agent systems via sliding mode control. *Asian J. Control* **2024**, *26*, 1–14. [\[CrossRef\]](#)
6. Faghihi, F.; Cai, S.Q.; Moustafa, A.A. A neuroscience-inspired spiking neural network for EEG-based auditory spatial attention detection. *Neural Netw.* **2022**, *152*, 555–565. [\[CrossRef\]](#)
7. Lakshmanan, S.; Prakash, M.; Lim, C.P.; Rakkiyappan, R.; Balasubramaniam, P.; Nahavandi, S. Synchronization of an inertial neural network with time-varying delays and its application to secure communication. *IEEE Trans. Neural Netw. Learn. Syst.* **2018**, *29*, 195–207. [\[CrossRef\]](#)
8. Tang, C.; Li, X.Q.; Wang, Q. Mean-field stochastic linear quadratic optimal control for jump-diffusion systems with hybrid disturbances. *Symmetry* **2024**, *16*, 642. [\[CrossRef\]](#)
9. Zhang, D.Z.; Sun, W.F.; Dai, Y.S.; Bu, S.S.; Feng, J.H.; Huang, W.M. Intelligent kick detection using a parameter adaptive neural network. *Geoenergy Sci. Eng.* **2024**, *234*, 212694. [\[CrossRef\]](#)
10. Shi, K.B.; Cai, X.; She, K.; Wen, S.P.; Zhong, S.M.; Park, P.; Kwon, O.-M. Stability analysis and security-based event-triggered mechanism design for T-S fuzzy NCS with traffic congestion via DoS attack and its application. *IEEE Trans. Fuzzy Syst.* **2023**, *31*, 3639–3651. [\[CrossRef\]](#)
11. Kong, F.C.; Zhu, Q.X.; Huang, T.W. New fixed-time stability lemmas and applications to the discontinuous fuzzy inertial neural networks. *IEEE Trans. Fuzzy Syst.* **2021**, *29*, 3711–3722. [\[CrossRef\]](#)
12. Fan, H.G.; Yi, C.B.; Shi, K.B.; Chen, X.J. Asymptotic synchronization for Caputo fractional-order time-delayed cellular neural networks with multiple fuzzy operators and partial uncertainties via mixed impulsive feedback control. *Fractal Fract.* **2024**, *8*, 564. [\[CrossRef\]](#)
13. Wang, S.T.; Shi, K.B.; Wang, J.; Yu, Y.B.; Wen, S.P.; Yang, J.; Han, S. Synchronization sampled-data control of uncertain neural networks under an asymmetric Lyapunov-Krasovskii functional method. *Expert Syst. Appl.* **2024**, *239*, 122475. [\[CrossRef\]](#)
14. Zhang, H.; Cheng, J.S.; Zhang, H.M.; Zhang, W.W.; Cao, J.D. Quasi-uniform synchronization of Caputo type fractional neural networks with leakage and discrete delays. *Chaos Solitons Fractals* **2021**, *152*, 111432. [\[CrossRef\]](#)
15. Ding, D.; Tang, Z.; Park, J.H.; Wang, Y.; Ji, Z.C. Dynamic self-triggered impulsive synchronization of complex networks with mismatched parameters and distributed delay. *IEEE Trans. Cybern.* **2023**, *53*, 887–899. [\[CrossRef\]](#)
16. Fan, H.G.; Chen, X.J.; Shi, K.B.; Wen, H. Distributed delayed impulsive control for μ -synchronization of multi-link structure networks with bounded uncertainties and time-varying delays of unmeasured bounds: A novel Halanay impulsive inequality approach. *Chaos Solitons Fractals* **2024**, *186*, 115226. [\[CrossRef\]](#)
17. Fu, Q.H.; Zhong, S.M.; Jiang, W.B.; Xie, W.Q. Projective synchronization of fuzzy memristive neural networks with pinning impulsive control. *J. Frankl. Inst.* **2020**, *357*, 10387–10409. [\[CrossRef\]](#)
18. Wang, S.T.; Shi, K.B.; Cao, J.D.; Wen, S.P. Fuzzy adaptive event-triggered synchronization control mechanism for T-S fuzzy RDNNs under deception attacks. *Commun. Nonlinear Sci. Numer. Simul.* **2024**, *134*, 107985. [\[CrossRef\]](#)
19. Duan, L.; Wei, H.; Huang, L.H. Finite-time synchronization of delayed fuzzy cellular neural networks with discontinuous activations. *Fuzzy Sets Syst.* **2019**, *361*, 56–70. [\[CrossRef\]](#)
20. Li, X.F.; Zhang, W.B.; Fang, J.A.; Li, H.Y. Finite-time synchronization of memristive neural networks with discontinuous activation functions and mixed time-varying delays. *Neurocomputing* **2019**, *340*, 99–109. [\[CrossRef\]](#)
21. Fan, H.G.; Chen, X.J.; Shi, K.B.; Liang, Y.H.; Wang, Y.; Wen, H. Mittag-Leffler synchronization in finite time for uncertain fractional-order multi-delayed memristive neural networks with time-varying perturbations via information feedback. *Fractal Fract.* **2024**, *8*, 422. [\[CrossRef\]](#)
22. Bao, H.B.; Park, J.H.; Cao, J.D. Exponential synchronization of coupled stochastic memristor-based neural networks with time-varying probabilistic delay coupling and impulsive delay. *IEEE Trans. Neural Netw. Learn. Syst.* **2016**, *27*, 190–201. [\[CrossRef\]](#) [\[PubMed\]](#)
23. Sun, J.W.; Han, G.Y.; Zeng, Z.G.; Wang, Y.F. Memristor-based neural network circuit of full-function Pavlov associative memory with time delay and variable learning rate. *IEEE Trans. Cybern.* **2020**, *50*, 2935–2945. [\[CrossRef\]](#) [\[PubMed\]](#)
24. Wen, S.P.; Hu, R.; Yang, Y.; Huang, T.W.; Zeng, Z.G.; Song, Y.D. Memristor-based echo state network with online least mean square. *IEEE Trans. Syst. Man Cybern. Syst.* **2019**, *49*, 1787–1796. [\[CrossRef\]](#)
25. Ding, D.; Tang, Z.; Wen, C.B.; Ji, Z.C. Bipartite synchronization for coupled memristive neural networks: Memory-based dynamic updating law. *Knowl.-Based Syst.* **2024**, *299*, 112102. [\[CrossRef\]](#)
26. Hua, W.T.; Wang, Y.T.; Liu, C.Y. New method for global exponential synchronization of multi-link memristive neural networks with three kinds of time-varying delays. *Appl. Math. Comput.* **2024**, *471*, 128593. [\[CrossRef\]](#)
27. Li, R.X.; Cao, J.D. Stabilization and synchronization control of quaternion-valued fuzzy memristive neural networks: Nonlinear scalarization approach. *Fuzzy Sets Syst.* **2024**, *477*, 108832. [\[CrossRef\]](#)
28. Bao, H.B.; Cao, J.D. Projective synchronization of fractional-order memristor-based neural networks. *Neural Netw.* **2015**, *63*, 1–9. [\[CrossRef\]](#)
29. Bao, H.B.; Park, J.H.; Cao, J.D. Adaptive synchronization of fractional-order memristor-based neural networks with time delay. *Nonlinear Dyn.* **2015**, *82*, 1343–1354. [\[CrossRef\]](#)
30. Liu, S.X.; Yu, Y.G.; Zhang, S. Robust synchronization of memristor-based fractional-order Hopfield neural networks with parameter uncertainties. *Neural Comput. Appl.* **2019**, *31*, 3533–3542. [\[CrossRef\]](#)

31. Gu, Y.J.; Wang, H.; Yu, Y.G. Synchronization for commensurate Riemann-Liouville fractional-order memristor-based neural networks with unknown parameters. *J. Frankl. Inst.* **2020**, *357*, 8870–8898. [\[CrossRef\]](#)
32. Gu, Y.J.; Yu, Y.G.; Wang, H. Projective synchronization for fractional-order memristor-based neural networks with time delays. *Neural Comput. Appl.* **2019**, *31*, 6039–6054. [\[CrossRef\]](#)
33. Fan, H.G.; Rao, Y.; Shi, K.B.; Wen, H. Time-varying function matrix projection synchronization of Caputo fractional-order uncertain memristive neural networks with multiple delays via mixed open loop feedback control and impulsive control. *Fractal Fract.* **2024**, *8*, 301. [\[CrossRef\]](#)
34. Yan, H.Y.; Qiao, Y.H.; Ren, Z.H.; Duan, L.J.; Miao, J. Master-slave synchronization of fractional-order memristive MAM neural networks with parameter disturbances and mixed delays. *Commun. Nonlinear Sci. Numer. Simul.* **2023**, *120*, 107152. [\[CrossRef\]](#)
35. Yang, X.J.; Li, C.D.; Huang, T.W.; Song, Q.K.; Huang, J.J. Synchronization of fractional-order memristor-based complex-valued neural networks with uncertain parameters and time delays. *Chaos Solitons Fractals* **2018**, *110*, 105–123. [\[CrossRef\]](#)
36. Kao, Y.G.; Li, Y.; Park, J.H.; Chen, X.Y. Mittag-Leffler synchronization of delayed fractional memristor neural networks via adaptive control. *IEEE Trans. Neural Netw. Learn. Syst.* **2021**, *32*, 2279–2284. [\[CrossRef\]](#)
37. Yang, S.; Yu, J.; Hu, C.; Jiang, H.J. Finite-time synchronization of memristive neural networks with fractional-order. *IEEE Trans. Syst. Man Cybern. Syst.* **2021**, *51*, 3739–3750. [\[CrossRef\]](#)
38. Li, H.L.; Cao, J.D.; Hu, C.; Jiang, H.J.; Alsaedi, A. Synchronization analysis of nabla fractional-order fuzzy neural networks with time delays via nonlinear feedback control. *Fuzzy Sets Syst.* **2024**, *475*, 108750. [\[CrossRef\]](#)
39. Li, H.L.; Cao, J.D.; Hu, C.; Zhang, L.; Jiang, H.J. Adaptive control-based synchronization of discrete-time fractional-order fuzzy neural networks with time-varying delays. *Neural Netw.* **2023**, *168*, 59–73. [\[CrossRef\]](#)
40. Du, F.F.; Lu, J.G. Adaptive finite-time synchronization of fractional-order delayed fuzzy cellular neural networks. *Fuzzy Sets Syst.* **2023**, *466*, 108480. [\[CrossRef\]](#)
41. Du, F.F.; Lu, J.G.; Zhang, Q.H. Practical finite-time synchronization of delayed fuzzy cellular neural networks with fractional-order. *Inf. Sci.* **2024**, *667*, 120457. [\[CrossRef\]](#)
42. Jin, W.B.; Cui, W.X.; Wang, Z.J. Finite-time synchronization of fractional-order complex-valued fuzzy cellular neural networks with time-varying delays. *J. Intell. Fuzzy Syst.* **2021**, *41*, 7341–7351. [\[CrossRef\]](#)
43. Podlubny, I. *Fractional Differential Equations*; Academic Press: New York, NY, USA, 1999.
44. Du, F.F.; Lu, J.G. Finite-time synchronization of fractional-order delayed fuzzy cellular neural networks with parameter uncertainties. *IEEE Trans. Fuzzy Syst.* **2023**, *31*, 1769–1779. [\[CrossRef\]](#)
45. Chen, B.S.; Chen, J.J. Global asymptotical ω -periodicity of a fractional-order non-autonomous neural networks. *Neural Netw.* **2015**, *68*, 78–88. [\[CrossRef\]](#)
46. Bhalekar, S.; Gejji, V. A predictor-corrector scheme for solving nonlinear delay differential equations of fractional order. *J. Fract. Calc. Appl.* **2011**, *1*, 1–9.

Disclaimer/Publisher’s Note: The statements, opinions and data contained in all publications are solely those of the individual author(s) and contributor(s) and not of MDPI and/or the editor(s). MDPI and/or the editor(s) disclaim responsibility for any injury to people or property resulting from any ideas, methods, instructions or products referred to in the content.